2020 10th Advanced Satellite Multimedia Systems Conference and the 16th Signal Processing for Space Communications Workshop (ASMS/SPSC)

DOI: 10.1109/ASMS/SPSC48805.2020.9268819

# A Flexible OFDM-Like DFT-s-OFDM Reference Symbol

Arnaud Bouttier

# A Flexible OFDM-like DFT-s-OFDM Reference Symbol

Arnaud Bouttier
Mitsubishi Electric R&D Centre
Europe (MERCE)
Rennes, France
a.bouttier@fr.merce.mee.com

*Abstract*— **With many high throughput satellites (HTS) in space, the satellite industry is now able to provide flexible services at costs that tend to become competitive. Satellite networks may ultimately play a significant role in the global telecommunication market. As an illustration of this trend, satellite stakeholders are pushing with some success for a satellite component in the global 5G system. With power fluctuations similar to those of single carrier waveforms, the discrete Fourier transform spread orthogonal frequency division multiplexing (DFT-s-OFDM) modulation appears as a relevant waveform for some satellite applications such as backhauling. Despite its many advantages, DFT-s-OFDM still lacks of reference signals (RS) showing low-power fluctuations for whatever length. In this paper, we propose a new RS that consists in inserting an OFDM pilot with its own cyclic prefix within a DFT-s-OFDM symbol. The novelty is here to modulate specific samples that are computed to closely match - after modulation - the OFDM pilot thus minimizing the interference resulting from the insertion. Performance evaluations assess the relevance of the proposed scheme that brings the flexibility of OFDM RS to DFT-s-OFDM systems.**

***Keywords—DFT-s-OFDM, satellite, SC-OFDM, 5G, RS, pilot***

## I. INTRODUCTION

The satellite communications (SatCom) industry has undergone massive changes since the deployment of high-throughput satellites (HTS) over the last decades. With much more flexible and affordable resources, SatCom may ultimately gather a larger part of the global communication market. Further changes may also result from the launch of large low Earth orbit (LEO) satellites constellations within the coming years. As an acknowledgment of this new paradigm, the 3GPP has recently initiated standardization activities in the purpose of including a satellite component in the future releases of the 5G system [1].

It is likely that SatCom will enter 5G starting from the upper protocol layers in order to facilitate the deployment of existing applications such as backhauling and truncking. These systems may rely at first on the widely deployed and proven DVB-S2x protocol [2] for the actual transmission of radio signals between satellites and ground equipment. If the DVB-S2x time division multiplex (TDM) modulation is well suited for applications such as linear TV, it suffers from some limitations when it comes to transmit data in a cellular and possibly mobile context, starting with a time-only duplexing access scheme and the need for large guard periods between signals coming from different sources.

It might thus be required in the future to adapt existing physical layers - or even design new ones - specifically for satellite transmissions, either within or outside 3GPP. The orthogonal frequency division (OFDM) multiplexing modulation appears as the most relevant candidate thanks to its versatility. It is actually standardized in satellite systems such as DVB-H, -SH and -NGH [3]. However, in power-constrained situations, the large peak to average power ratio (PAPR) of OFDM signals may lead to performance degradations due to saturation effects in power amplifiers. Another solution would be to rely on the DFT-s-OFDM modulation, a transmission scheme that is already used in the uplink of the 3GPP/LTE system [4] and was also standardized in the DVB-NGH system [5].

The DFT-s-OFDM modulation actually combines some key advantages of both the OFDM and TDM techniques. Just like in TDM, the DFT-s-OFDM modulation shapes the samples to be transmitted with a waveform that is here the Dirichlet kernel [8], the discrete time Fourier transform (DTFT) of the window function. However, unlike in TDM, the filtering is applied circularly over a finite block of samples. From that respect, the DFT-s-OFDM modulation can be considered as a block implementation of the TDM modulation thus benefiting from the same low PAPR. This also enables multiplexing in time several signals without the need of large guard periods.

The OFDM leg of the DFT-s-OFDM modulation makes it suitable for transmissions over degraded channels thanks to an equalization natively applied in the frequency domain. This is actually possible as long as a cyclic prefix (CP) is inserted, also leading to a better robustness to time synchronization errors. If the DFT-s-OFDM modulation benefits from its OFDM lineage for the equalization, it is not the case for the insertion of reference symbols (RS) required for channel estimation. Indeed, the low power fluctuations of its envelope result from the application of an IDFT on previously DFT-spread samples. Any arbitrary alteration of the DFT-spread sub-carriers through for instance the insertion of known sub-carriers breaks the PAPR properties of the signal.

In this paper, we propose a new reference symbol that exhibits a low PAPR whatever its length. This is obtained by inserting an OFDM symbol within a DFT-s-OFDM symbol with a limited impact on the demodulation of the embedded data. This paper is organized as follows: The next section provides a description of the related work. In Section III, we introduce the principle of the proposed scheme which is formally described in Section IV. Section V provides simulation results and in Section VI a conclusion is given.

## II. RELATED WORK

In order to keep low the PAPR, the 3GPP/LTE uplink system generates a full pilot, i.e. where all the sub-carriers of the OFDM symbol carry reference samples, actually a Zadoff-Chu sequence (ZC, [6]) that exhibits a low PAPR after modulation. In order to reduce the pilot overhead, the DVB-NGH system specifies the PP9 pilot [5] that interleaves an equal number of data and reference samples in the frequency domain. The resulting signal that is the sum of two consecutive replica of two independent SC signals is no more a pure SC signal but still shows a good PAPR. With an equal ratio of data and pilot samples, the PP9 RS is especially well suited for channels with very large power delay spread and or Doppler. It is however over-dimensioned for less degraded channels.

In [7], the authors introduced a new pilot scheme denoted as time division multiplex pilot (TDMPi). In this scheme, the reference symbol is modulated like any other DFT-s-OFDM symbol. The vector of samples to be transmitted is divided into two parts: a front part containing an arbitrary number of reference samples known at the receiver and a second part containing information data. The principle is here to generate a symbol that contains a fixed pattern to be used by the receiver as a pseudo-OFDM RS. In order to reduce the interference of the data onto the pilot due to Dirichlet filtering, the TDMPi scheme modulates separately pilots and data and the contribution of data samples onto the pilot part is zeroed before combining the two modulated signals.

A key advantage of this approach is that the zeroing operation does not degrade the PAPR whatever the length of the pilot. Another key feature of the TDMPi scheme is the insertion of the so-called pilot cyclic prefix (PCP), i.e. a CP not related to the overall symbol but to the pilot part. The objective is here to favor the quality of the channel estimation in situations where a few RS are inserted in the modulated frames. It is then possible to demodulate data-only symbol using a good channel estimate while only the data carried within the RS suffer from some degradations. These samples indeed suffer from two detrimental effects: the destruction of the OFDM orthogonality due to the zeroing operation and the lack of circularity due to the insertion of the PCP.

The lack of a global CP may also lead to the loss of information about the last samples in the symbol when the demodulation FFT window is positioned a few samples back in the CP, e.g. due to synchronization errors or on purpose to be more robust against rapidly varying channels. It shall also be mentioned that the reference symbol used for estimating the channel is not a true OFDM symbol, thus leading to some degradations in channel estimation when using OFDM-based methods. Overall, if the TDMPi scheme is well suited for power-constrained and quasi-stationary contexts, there is still the need for a more versatile scheme.

## III. PROPOSED SCHEME

In this paper, we propose a new reference symbol that consists in inserting a truly OFDM-modulated pilot including its dedicated CP within a DFT-s-OFDM symbol. An obvious advantage of this solution is that both the reference and the overall symbols are protected by their own CP, getting rid of the PCP issue in the TDMPi scheme. Another benefit is the possibility to rely on any existing technique for generating the OFDM pilot but also for estimating the channel. One may argue that the OFDM symbol could be inserted as a separate symbol within the flow of data-only symbols. The rational for inserting it into a data symbol is to keep unchanged the frame structure whatever the length of the pilot that might be variable in time.

It is rather obvious that the introduction of external samples within a DFT-s-OFDM modulated symbol cannot be seamless. A straightforward implementation of the new RS would be to replace some samples of a DFT-s-OFDM modulated symbol by new samples, operation that can be interpreted as an initial zeroing followed by the actual insertion of new samples (another one would be to modulate a small symbol and insert new samples between two original ones). Just like for the TDMPi RS, a way to reduce the impact of the insertion is to introduce zeros in the original data stream at the positions corresponding to the samples to be replaced – called here the pilot region. However, this simply reduces the level of degradations due to zeroing as the analogue signal is null only at the positions of the zeros but not elsewhere.

The data samples obtained after demodulation also contain an unwanted interference originating from the insertion of the external samples. Forcing the corresponding samples to zero prior demodulation would not be satisfactory in case of synchronization error or channel dispersion. The originality of the new scheme actually relies in the methodology used to reduce the interference resulting from the insertion when demodulating the data embedded in the RS. Interestingly, the proposed scheme also reduces the level of out-of-band (OOB) radiations that may result from the amplitude breaks at the interface between the DFT-s-OFDM symbol and the inserted OFDM symbol.

The principle of the proposed scheme is to introduce specific pilot samples in the original block of data computed in such a way that the samples obtained after modulation closely resemble to the ones of the OFDM pilot. If the modulated samples would perfectly match with the inserted ones, there would be no degradations resulting from the insertion. This is obviously impossible, as the OFDM symbol cannot be obtained as the result of a DFT-s-OFDM modulation. However, simulations show that it is possible to significantly reduce the degradation in comparison to the basic zeroing operation. As these samples are not meant to be used at the receiver, they are conveniently denoted here as ghost pilots. Fig. 1 depicts the general principle of the proposed scheme that is described hereafter as the ghost-based reference symbol (GbRS).

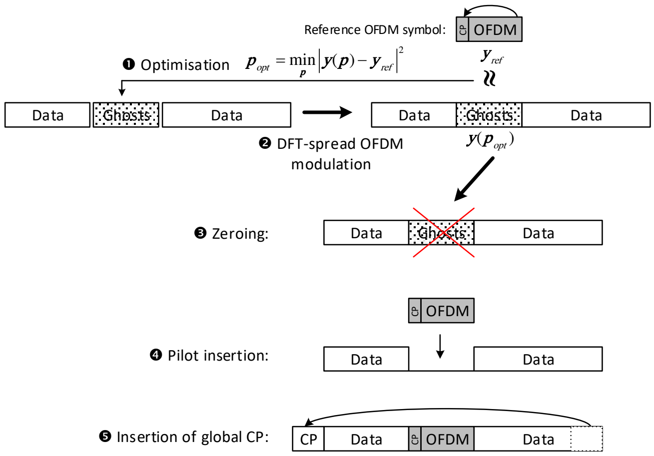


Fig. 1. Principle of the GbRS reference symbol.

## IV. Description

### A. Computation of the GbRS

The proposed technique is best introduced using the matrix description of the DFT-s-OFDM modulation. Over each symbol period, the modulated symbols carry $K$ time-domain samples oversampled by a factor $N/K$ with the addition of $P$ null sub-carriers on both edges of the multiplex ($N=K+2P$). Let us denote $x_k$ the data samples which are parsed into blocks of $K$ samples $\boldsymbol{x} = [x_0, \dots, x_{K-1}]^t$ over each symbol period. Each data block $\boldsymbol{x}$ is first spread in frequency using a $K$-point normalized Discrete Fourier Transform (DFT) such as

$$\boldsymbol{x}_f = A\boldsymbol{x} \text{ where } A = P_c F_K \quad (1)$$

In (1) $P_c$ is the ($K$, $K$) permutation matrix that swaps the two halves of each column of the matrix it is applied to, and where $F_K$ is the $K$-point normalized DFT under the form of a ($K$, $K$) matrix with elements $F_{k,n} = w_K^{kn}/\sqrt{K}$ on the $k^{\text{th}}$ row and $n^{\text{th}}$ column, $w_K = \exp(2j\pi/K)$ being a primitive root of unity. After spreading and addition of the null sub-carriers, the samples are OFDM modulated using the ($N$, $K$) matrix

$$B = P_r F_N^* \times \sqrt{N/K}, \quad (2)$$

where $P_r$ is the ($N$, $N$) permutation matrix that swaps the two halves of each row of the matrix it is applied to, and where $F_N^* = F_N^{-1}$ is the $N$-point normalized inverse DFT (IDFT). In this matrix, we keep only the contribution of the spread data ignoring the null sub-carriers

$$B_m = B(\,0{:}\,N-1, P{:}\,N-P-1). \quad (3)$$

Finally, the modulated signal can be computed as

$$\boldsymbol{y} = \mathrm{C}\boldsymbol{x} \text{ where } C \triangleq B_m A. \quad (4)$$

In the case of the reference symbol, $\boldsymbol{x}$ embeds both information data denoted as $d_k$ and ghost pilots denoted as $p_k$ which position is defined according to the size and position of the OFDM pilot to be inserted. It is assumed here the OFDM pilot is made of $R$ samples extended with a CP with length $L$ leading to a total number of samples $S = R + L$. This vector, denoted as $\boldsymbol{y}_{ref}$ in the sequel, shall be generated to show low power fluctuations. A typical but not restrictive solution is to rely on the so-called Zadoff-Chu sequences. Note that the length of the CP does not need to be necessarily the same for the OFDM pilot and the overall reference symbol. For simplification, they are assumed equal here with a length greater than the channel delay spread.

The OFDM pilot can be inserted in whatever position within the DFT-s-OFDM reference symbol. We assume here that the first sample of the OFDM symbol is inserted at the index $T_1$ in [0, $N$-1]. The last sample of the OFDM pilot is thus inserted at the index $T_2 = T_1 + S - 1$. The index of the first and last ghost samples are then obtained as

$$J_1 = \left[T_1 \times \frac{K}{N}\right]^- - w_1, J_2 = \left[T_2 \times \frac{K}{N}\right]^+ + w_2, \quad (5)$$

$[.]^-$ and $[.]^+$ being respectively the rounding down and up to the nearest integer functions and $w_1$ and $w_2$ two unsigned integers. Equation (5) shows that at least one ghost sample lies on each side of the OFDM pilot (all the original discrete samples belong to the generated analogue signal). This is required to facilitate the matching between the modulated samples and the inserted ones.

Globally, the original vector to be modulated is divided into three parts, a front part with length $K_1 = J_1$, a central part with length $G = J_2 - J_1 + 1$ and a rear part with length $K_2 = K - K_1 - G$. The total number of data carried out by the front and rear parts in the original vector is denoted as $K_d = K_1 + K_2$. After modulation, the signal is also sliced into three parts made respectively of $N_1 = T_1$, $S$ and $N_2 = N - N_1 - S$ samples.

Our goal is to compute the vector of ghost pilots such that the signal generated over the interval $[T_1, T_2]$ closely mimics the value of the OFDM symbol to be inserted afterwards. Let us denote by $\boldsymbol{p} = [p_0, \dots, p_{G-1}]^t$ the vector of ghost pilot samples populating the central part of the vector $\boldsymbol{x}$. For convenience, the set of information data within $\boldsymbol{x}$ is grouped as a single vector with length $K_d$ denoted by $\boldsymbol{d} = [d_0, \dots, d_{K_d-1}]^t$. After modulation, the value of the signal in the central part depends not only on the ghost pilots but also on the surrounding data. Let us first compute the contribution of the useful data onto the central part of the generated signal. The spreading step is computed using the matrix $A$ in (1) taking into account only the useful data

$$A_d = A(0{:}\,K-1, 0{:}\,J_1 - 1 \cup J_2 + 1{:}\,K-1). \quad (6)$$

After spreading and addition of the null sub-carriers, the samples are OFDM modulated using the matrix $B_m$ in (3) where we keep only the samples of the central part

$$B_{pm} = B(N_1{:}\,N_2, P{:}\,N-P-1). \quad (7)$$

Overall, the contribution of the front and rear parts of the original vector to the central part of the generated signal is obtained from the $(S, K_d)$ matrix

$$C_{pd} = B_{pm} A_d \quad (8)$$

Similarly, the contribution of the ghost pilots on the central part of the generated signal is obtained from the $(S, G)$ matrix

$$C_{pp} = B_{pm} A_p, \quad (9)$$

where $A_p = A(0{:}\,K-1, J_1{:}\,J_2)$. The set of ghost pilot samples that mimics the OFDM pilot symbol can thus be obtained as the solution of the following linear system

$$C_{pp}\boldsymbol{p} = \boldsymbol{y}_{ref} - C_{pd}\boldsymbol{d}. \quad (10)$$

As the matrix $C_{pp}$ is full rank and has more rows than columns, the corresponding system has no exact solution. It is common in such a case, to compute the least-squares solution

$$\boldsymbol{p}_{opt} = \min_{\boldsymbol{p}} \left\| C_{pp}\boldsymbol{p} - \boldsymbol{y}_{ref} + C_{pd}\boldsymbol{d} \right\|_2^2. \quad (11)$$

Experiments show that the ghost samples falling outside the pilot region tend to take large values to improve the matching (they appear on purpose as degrees of freedom in the system). It is thus better to apply the optimization with a constraint, e.g. over the amplitude, in order not to degrade the overall PAPR.

As long as the length of the OFDM pilot is small, i.e. a few tens of samples, the complexity of the system in (10) remains acceptable. For longer pilots, it is possible to reduce the complexity e.g. by enforcing the matching over a limited number of samples on both sides. This solution enables to build an under-determined system leading to a better match for the samples and thus reduced OOB radiations. However, the number of ghost samples remains identical and possibly large. Another alternative is to compute a limited number of ghost samples on each side of the pilot region. The level of performance appears to be degraded but with a better matching on both sides. These two approaches have been successfully tested but only the original one is addressed in this paper.

### *B. Channel Estimation*

It is assumed here that the receiver is synchronized and knows the position of the OFDM pilot symbol within the reference symbol. The receiver first extracts $L$ samples from the OFDM pilot ideally just after the end of the cyclic prefix. Let us denote $\boldsymbol{u} = [u_0, \dots, u_{P-1}]^t$ the vector of samples with length $P$ used to generate the OFDM pilot. It is assumed that the samples are DFT ordered with positive frequencies coming first. The channel is supposed to be linear time invariant (LTI) with a delay spread shorter than the CP. The signal received over a given symbol period is given by

$$\boldsymbol{z}_f = C_L(\boldsymbol{h}_L)\boldsymbol{y}_f + \boldsymbol{b} = \sqrt{L/P}\, C_L(\boldsymbol{h}_L) F_L^* Q \boldsymbol{u} + \boldsymbol{b}, \quad (12)$$

where $\boldsymbol{h}_L$ is the discrete time band-limited baseband channel impulse response of the channel with length $L$, $C_L(\boldsymbol{h}_L)$ the circulant filtering matrix associated to $\boldsymbol{h}_L$ and $\boldsymbol{b}$ an additive white Gaussian noise (AWGN) with variance $\sigma^2$ and $Q$ the matrix that inserts null sub-carriers in the center of the multiplex. After OFDM demodulation, we obtain

$$\boldsymbol{w}_f = \sqrt{P/L}\, Q^\dagger F_L \boldsymbol{z}_f = Q^\dagger diag\left(\sqrt{L} F_L \boldsymbol{h}_L\right) Q \boldsymbol{u} + \boldsymbol{b}',$$

$$\boldsymbol{w}_f = Q^\dagger diag\left(\boldsymbol{h}_L^f\right) Q \boldsymbol{u} + \boldsymbol{b}' = diag\left(\boldsymbol{h}_P^f\right) \boldsymbol{u} + \boldsymbol{b}', \quad (13)$$

where we use the well-known properties of circulant and Fourier matrices [9]. In (13) $Q^\dagger$ is the matrix that extracts the modulated sub-carriers, $\boldsymbol{h}_L^f$ the $L$-point non-normalized DFT of the vector $\boldsymbol{h}_L$ and $\boldsymbol{h}_P^f$ the result of the extraction of the channel response for the modulated sub-carriers only [10]. As it is well known in CP-OFDM, the demodulation simply requires the estimation of $P$ channel coefficients in the DFT frequency domain. Here, the channel is estimated directly for the $K$ coefficients according to the linear minimum mean square error (MMSE) criterion. We look for the channel coefficients such that

$$\widehat{\boldsymbol{h}}_K^f = H_{opt} \boldsymbol{w}_f,$$

with

$$H_{opt} = arg \min_H E\left|H \boldsymbol{w}_f - \boldsymbol{h}_K^f\right|^2, \quad (14)$$

where $\boldsymbol{h}_K^f$ is the vector of channel coefficients over the $K$ modulated sub-carriers and $H$ a ($K$, $L$) weighting matrix. Under the retained assumptions, one can easily show that the MMSE estimator is given by

$$H_{opt} = R_{\boldsymbol{h}_K^f \boldsymbol{w}_f} R_{\boldsymbol{w}_f \boldsymbol{w}_f}^{-1}, \quad (15)$$

$R_{\boldsymbol{xy}}$ being the correlation matrix between the vectors $\boldsymbol{x}$ and $\boldsymbol{y}$. Using the observation vector $\boldsymbol{u}_f$ in (13) we obtain

$$\begin{cases} R_{\boldsymbol{h}_K^f \boldsymbol{w}_f} = R_{\boldsymbol{h}_K^f \boldsymbol{h}_P^f} S_P^H \; with \; S_P = diag(\boldsymbol{u}^*), \\ R_{\boldsymbol{w}_f \boldsymbol{w}_f} = (\boldsymbol{s}\boldsymbol{s}^H) \odot R_{\boldsymbol{h}_P^f \boldsymbol{h}_P^f} + I_P \sigma^2, \end{cases} \quad (16)$$

where $I_P$ is the identity matrix with size $P$. In the present case, the channel power delay profile is assumed to be perfectly known. In practice, the correlation matrices are computed empirically from the observations or set to a predefined value.

## V. PERFORMANCE ANALYSIS

The performance of the GbRS scheme is analyzed here by means of simulations. Performance is measured in terms of instantaneous normalized power (INP) for signal envelope, mean square error (MSE) for channel estimation and error vector magnitude (EVM) for demodulation. Bit error rate is not evaluated as coding may "hide" weak behaviors. We consider a satellite context where the channel delay spread is fairly small with respect to the symbol duration. The number of modulated sub-carriers is set to $K$=432 for a total number of $N$=512 sub-carriers (DVB-NGH parameters for a 5 MHz bandwidth). The CP is set to $L$=32 for both the global symbol and the OFDM symbol. The pilot samples prior to DFT are obtained as the IDFT of ZC sequences selected for each tested size $S$. The data samples are modulated according to a robust quaternary phase shift keying (QPSK) constellation.

### *A. Signal envelope performance*

At first, the PAPR and more precisely the complementary cumulative distribution function (CCDF) of the instantaneous normalized power (INP) have been measured with an oversampling factor of 8 for different lengths $S$ = 40, 80, 120, 160, 200, i.e. covering sizes up to almost half the symbol length. Fig. 2 compares the measured INP CCDFs with the amplitude distribution of a data-only DFT-s-OFDM symbol modulated in QPSK. These curves confirm that the GbRS behaves similarly to data symbols whatever the length of the pilot region. Note that the CCDF of the reference symbol is even slightly better thanks to the low PAPR of the inserted OFDM pilot.

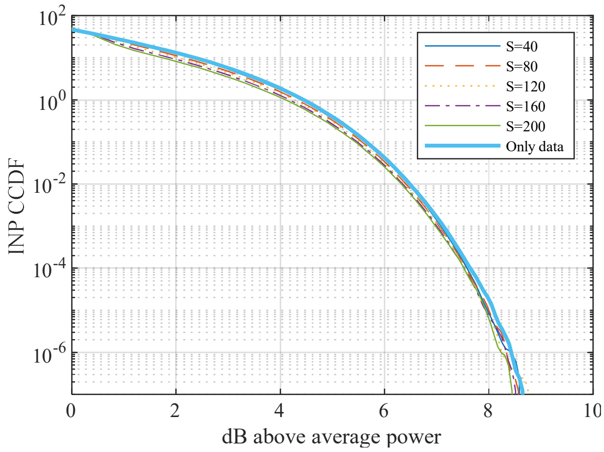


Fig. 2. CCDF of the INP for different sizes.

Fig. 3 illustrates qualitatively the degree of matching between the inserted OFDM symbol and the signal generated using the ghost samples. The figure actually focuses on the first samples of the pilot region for a signal generated with the following parameters: $T_1 = 24, S = 30, L = 20, w_1 = w_2 = 0$, and a saturation value of $A_{max} = 1.4$ for the ghost pilots amplitude. Logically, the signal generated from the ghost samples does not strictly match with the inserted samples but globally reproduces its shape. It can be noticed in this particular case that the first samples of both signals closely match. This demonstrates the interest of introducing a ghost sample outside the pilot region to improve amplitude matching but also to reduce the OOB radiations resulting from the insertion.

### B. *Cost of the OFDM pilot insertion*

Let's now evaluate quantitatively the impact of inserting the OFDM symbol in place of the samples obtained from the ghost pilots. This is achieved by measuring the error vector magnitude (EVM) of the demodulated samples, i.e. the root mean square (RMS) average amplitude of the error vector, normalized to the ideal signal amplitude reference. The EVM is computed here not as a single number for the whole symbol but as a function of the position of the samples in the vector. As shown later, the error indeed depends on the position of the sample with a larger error close to the pilot region. At first, the EVM is computed under the assumption of an ideal channel (no multipath and no noise), perfect channel estimation, and MMSE equalization followed by a de-normalization stage as described in [10].

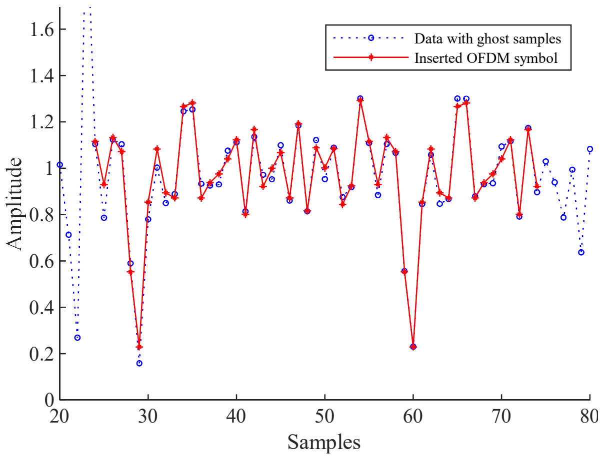


Fig. 3. Illustration of the matching obtained with the ghost pilots.

Fig. 4 compares the EVM obtained with the TDMPi RS and the GbRS for different lengths. As previously explained, the computation of the ghost samples requires the application of a constraint on the amplitude that is especially relevant on the edges. For that reason, the OFDM pilot is inserted with a circular shift (prior CP insertion) which value is selected to minimize the EVM. In addition, the OFDM symbol is inserted at the index $T_1$ that minimizes the EVM (it is in general better that the first ghost samples on both edges fall close to the middle between two OFDM samples). Fig. 4 shows that the proposed solution reduces the level of interference over the data symbol especially on the edges thanks to the matching operation. As shown in the sequel, the reduction of the interference is much more significant in case of ISI.

Another alternative for reducing the level of interference is to insert more ghost pilots on each side of the pilot region. It appears that the level of interference can be reduced by a factor 2 at the expense of 1 or 2 more pilots on each side. The actual number of additional pilots shall be defined in terms of spectral efficiency, as the reduction of the interference may lead to an overall better spectral efficiency for large constellations.

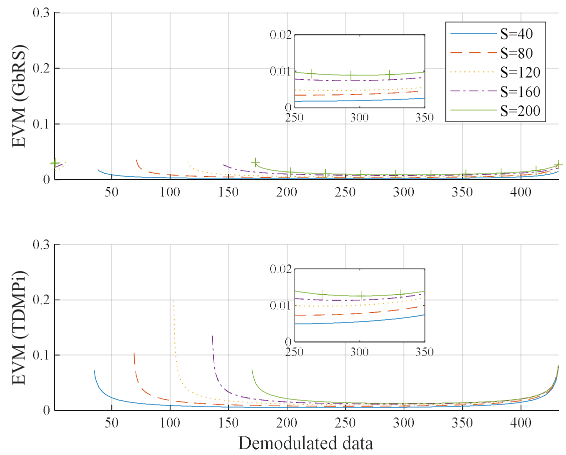


Fig. 4. Comparison of the EVM for different sizes (ideal channel).

### C. *Channel estimation performance*

We now focus on the evaluation of the GbRS in terms of channel estimation using the MMSE scheme described in Section IV. The performance is measured in terms of mean square error (MSE) with respect to the actual channel response in the frequency domain. The scheme was evaluated in the context of the AWGN and the 6-tap Rayleigh TU6 channels [11]. For the TU6 channel, the channel MSE was averaged over 50,000 realizations with a random selection of new channel coefficients for each tested reference symbol. In order to avoid degradation due to inter-symbol interference (ISI), the CP is set to $L$=32 samples (the channel spreads over 26 samples assuming tap delays fall on sampling times) for an overall length of $S$=64 for the OFDM pilot.

Fig. 5 compares the channel estimation MSE of the GbRS as compared to the TDMPi and an OFDM RS with the same size that would be transmitted separately from the DFT-s-OFDM symbols. Logically, the GbRS scheme shows similar performance to the pure OFDM symbol. Fig. 5 also shows that the MSE of the TDMPi is slightly above the OFDM case (here by only 0.1 dB). As explained in [7], the TDMPi performance can significantly depart from OFDM for some configurations which is the not the case for the new scheme. This is actually the main advantage of the GbRS: to bring OFDM RS performance to DFT-s-OFDM signals.

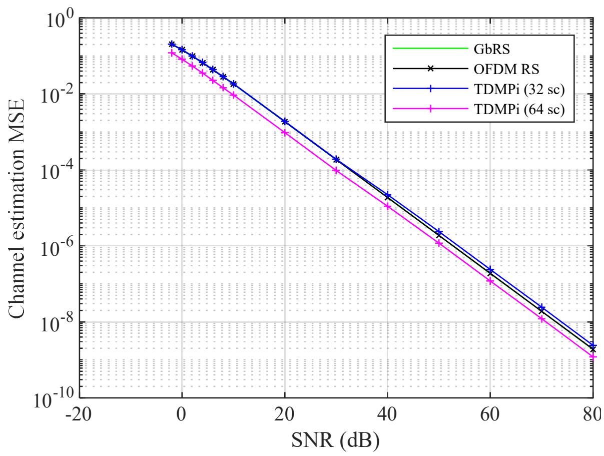


Fig. 5. Channel estimation MSE for the TU6 and AWGN channels.

### D. Demodulation performance

We now look at the impact of the channel estimation on the demodulation of the data samples embedded within the RS. It is important to remind that the TDMPi is able to carry more data samples for a given number of reference sub-carriers (same CP for pilot and overall symbol). Thus, the performance for the data part has been measured for the same number of data samples, i.e. with 64 reference sub-carriers for the TDMPi scheme and $R = 32$ for the new scheme (leading to 64 samples with the addition of the CP). The EVM is measured in terms of excursion (minimum and maximum values) as measured from the EVM averaged over each data position. Logically, the extension in the number of reference sub-carrier leads to better performance in terms of channel estimation (~2.8 dB) for the TDMPi. But as shown on Fig. 6, the EVM remains significantly better for the GbRS scheme. In case of channel delay spread, the lack of circularity due to the PCP strongly affects the TDMPi scheme. With a separate CP for the pilot and the overall symbol, the GbRS pilot suffers from less degradations. This is precisely the purpose of the GbRS: to provide an alternative to TDMPi for channels with large delay spreads.

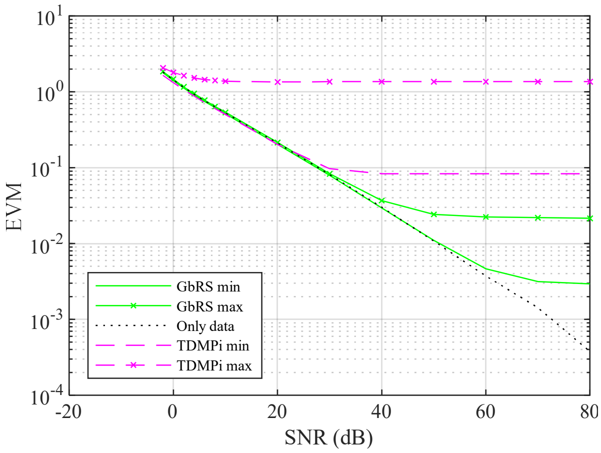


Fig. 6. Demodulation performance in EVM for the TU6 channel.

## VI. CONCLUSION

A novel reference symbol for the DFT-s-OFDM modulation is introduced in this paper. The principle is to insert an OFDM symbol within a DFT-s-OFDM symbol in such a way to minimize the interference generated by the insertion over the demodulated data. This is obtained by modulating the so-called ghost pilots so as to generate a signal that closely mimic the samples to be inserted at the same position. The main advantage is here to allow for using any OFDM channel estimation scheme whatever the length of the pilot still keeping low the power fluctuations. The so-called GbRS scheme exhibits three distinctive advantages: OFDM-like channel estimation performance, a limited level of degradation onto the embedded data and small out-of-band radiations. Besides further studies are required to simplify the linear system solving with constraints, the scheme appears as rather promising for satellites applications requiring a good robustness to channel degradations.

## REFERENCES


[1] 3GPP TR 22.822, "Study on using Satellite Access in 5G; Stage 1, (Release 16) ", June 2018.

[2] ETSI EN 302 307-2: "Digital Video Broadcasting (DVB); Second generation framing structure, channel coding and modulation systems for Broadcasting, Interactive Services, News Gathering and other broadband satellite applications; Part 2: S2-Extensions (S2X)," Oct. 2014.

[3] C. Ciochină-Duchesne, D. Castelain and A. Bouttier, "Satellite profile in DVB-NGH," *2012 6th Advanced Satellite Multimedia Systems Conference (ASMS) and 12th Signal Processing for Space Communications Workshop (SPSC)*, Baiona, 2012, pp. 182-188.

[4] 3GPP TS 36.300, "Evolved Universal Terrestrial Radio Access (E-UTRA) and Evolved Universal Terrestrial Radio Access (E-UTRAN); Overall description; Stage 2." http://www.3gpp.org.

[5] ETSI EN 303 105-1, "Digital Video Broadcasting (DVB); Next Generation broadcasting system to Handheld, physical layer specification (DVB-NGH); Part 1: Basic Profile," July 2017.

[6] Zepernick, Hans-Jürgen; Finger, Adolf. *Pseudo Random Signal Processing: Theory and Application*. Wiley, 2005.

[7] A. Bouttier and J. Guillet, "A low-PAPR low-pilot overhead Reference Signal for the DFT-spread OFDM Modulation," *2018 25th International Conference on Telecommunications (ICT)*, St. Malo, 2018, pp. 110-115.

[8] T. J. Cavicchi, "DFT time-domain interpolation," in *IEE Proceedings F - Radar and Signal Processing*, vol. 139, no. 3, pp. 207-211, June 1992.

[9] Davis, Philip J., Circulant Matrices, Wiley, New York, 1970.

[10] C. Ciochină, "Conception d'une couche physique pour la liaison montante dans des systèmes de radiocommunications mobiles cellulaires," PhD Thesis, July 2009.

[11] ETSI TR 101 290 V1.2.1 (2001-05). Technical report. *Digital Video Broadcasting (DVB), Measurement Guidelines for DVB Systems*. Technical Report ETSI, 2001.